ISSN 1674-1056
http://cpb.iphy.ac.cn
http://iopscience.iop.org/cpb
中国物理 B
Chinese Physics
中国物理
Chinese Physics B

Factors affecting improvement of fluorescence intensity of quartet and doublet state of NO diatomic molecule excited by glow discharge

Ahmed Asaad I Khalil, Reem Al-Tuwirqi, Mohammed A Gondal, Noura Al-Suliman

Citation: Chin. Phys. B . 2018, 27(8): 085202. **doi:** 10.1088/1674-1056/27/8/085202

Journal homepage: http://cpb.iphy.ac.cn; http://iopscience.iop.org/cpb

What follows is a list of articles you may be interested in

Numerical study on discharge characteristics influenced by secondary electron emission in capacitive RF argon glow discharges by fluid modeling

Lu-Lu Zhao(赵璐璐), Yue Liu(刘悦), Tagra Samir
Chin. Phys. B . 2018, 27(2): 025201. **doi:** 10.1088/1674-1056/27/2/025201

Effects of gas pressure on plasma characteristics in dual frequency argon capacitive glow discharges at low pressure by a self-consistent fluid model

Lu-Lu Zhao(赵璐璐), Yue Liu(刘悦), Tagra Samir
Chin. Phys. B . 2017, 26(12): 125201. **doi:** 10.1088/1674-1056/26/12/125201

Effect of driving frequency on electron heating in capacitively coupled RF argon glow discharges at low pressure

Tagra Samir, Yue Liu(刘悦), Lu-Lu Zhao(赵璐璐), Yan-Wen Zhou(周艳文)
Chin. Phys. B . 2017, 26(11): 115201. **doi:** 10.1088/1674-1056/26/11/115201

Numerical study on the gas heating mechanism in pulse-modulated radio-frequency glow discharge

Qi Wang(王奇), Xiao-Li Yu(于晓丽), De-Zhen Wang(王德真)
Chin. Phys. B . 2017, 26(3): 035201. **doi:** 10.1088/1674-1056/26/3/035201

Nitriding molybdenum： Effects of duration and fill gas pressure when using 100-Hz pulse DC discharge technique

U. Ikhlaq, R. Ahmad, M. Shafiq, S. Saleem, M. S. Shah, T. Hussain, I. A. Khan, K. Abbas, M. S. Abbas
Chin. Phys. B . 2014, 23(10): 105203. **doi:** 10.1088/1674-1056/23/10/105203

Factors affecting improvement of fluorescence intensity of quartet and doublet state of NO diatomic molecule excited by glow discharge*

Ahmed Asaad I Khalil[1,4,†], Reem Al-Tuwirqi[2], Mohammed A Gondal[3], and Noura Al-Suliman[4]

[1] Department of Laser Sciences and Interactions, National Institute of Laser Enhanced Sciences (NILES), Cairo University, Giza, 12613 Egypt
[2] Department of Physics, Faculty of Science, King Abdulaziz University, Jeddah 21551, Saudi Arabia
[3] Department of Physics, King Fahd University of Petroleum & Minerals, Dhahran 31261, Saudi Arabia
[4] Department of Physics, Faculty of Science for Girls, Imam Abdulrahman Ben Faisal University, Dammam 31441, Saudi Arabia

(Received 9 April 2018; revised manuscript received 18 May 2018; published online 25 July 2018)

We report on the observation of new fluorescence emission spectral transitions obtained from NO diatomic molecule in the region from ultraviolet (UV) to near infrared (NIR) in a low power glow discharge system. This glow discharge electronic excitation populates different quartet and doublet states of NO in its proximity such as the $A^2\Sigma$ ($\upsilon = 2$), $b^4\Sigma^-$ ($\upsilon = 3$), $B^2\Pi$ ($\upsilon = 4$), and $X^2\Pi$ ($\upsilon = 33$–32) states. Due to inter-system crossing, emission lines originating from these levels to lower lying states are recorded and spectral line assignments are performed. The observed systems include $b^4\Sigma^-$–$a^4\Pi$, $B^2\Pi$–$a^4\Pi$, $a^4\Pi$–$X^2\Pi$, $A^2\Sigma$–$X^2\Pi$, $X^2\Pi$–$X^2\Pi$ (33–15), $X^2\Pi$–$X^2\Pi$ (33–17), $X^2\Pi$–$X^2\Pi$ (33–20), and $X^2\Pi$–$X^2\Pi$ (33–18). This new information will conduce to the better understanding of the interesting features of NO molecule. Such parameters that affect the recording of low density of NO molecules are also discussed In addition to the factors such as the time evolution, argon gas concentration relative to NO mixture, the percentage of NO molecular gas concentration, discharge electric current signals and discharge applied voltage are studied. Those factors would enhance the fluorescence signal intensity of NO molecules. The recent results might be significant as reference data for optimizing the glow discharge spectrometer and diagnostics of NO gas.

Keywords: fluorescence emission, NO molecule, quartet states, intersystem crossing, glow discharge

PACS: 52.38.Mf, 52.25.Jm, 52.25.Kn, 42.55.Rz **DOI:** 10.1088/1674-1056/27/8/085202

1. Introduction

The importance of nitric oxide emerges from its diverse functions and roles. For example, NO molecule plays an important role in agriculture,[1] plants and bacteria,[2] and the atmosphere.[3] NO molecular emission from fuel combustion contributes to the greenhouse effect due to its contribution in increasing the level of troposphere ozone while depleting it from the stratosphere.[4] Moreover, NO molecule possesses an important function in the human body, which is conducive to regulating blood pressure, immune defense system, brain memory, and other functions.[5,6] Hence, the study of the NO molecule can be highly useful in many fields.

Due to these reasons, the nitrogen monoxide molecule has been investigated intensively, both experimentally and theoretically, in the past years.[7–14] The spectra included bands in the radio wave, microwave, infrared, visible and UV regions. The wealth of information aids in giving a complete and detailed picture of the electronic structure of NO beyond its first ionization limit.

The fluorescence of the γ, ε, and δ systems of NO molecule have been previously studied.[15] The fluorescence intensity spectra under applied electromagnetic waves with high resolution conduce to the understanding the electronic structure of NO molecule.[16–18] A prominent feature of the NO molecule is the fluorescence of the $A^2\Sigma$–$X^2\Pi$ system by UV radiation in the atmosphere.[19] In addition, the observing of the emission spectrum of NO molecule by glow discharge excitation is an important tool for studying the chemistry of the atmosphere and the environmental pollution.

Another important feature investigated in this study is the observation of quartet states of the NO molecule, such as the $a^4\Pi$ and the $b^4\Sigma^-$. The quartet $a^4\Pi$ state is the lowest excited state and plays an important role in rearranging the ground state atoms O ^{3}(P) and N ^{4}(S). Another interesting feature for the NO molecule is the crossing of the quartet $a^4\Pi$ state with the doublet $A^2\Sigma$ and the crossing of the quartet $b^4\Sigma^-$ with both the doublet states $A^2\Sigma$ and $B^2\Pi$. These states crossing can predict the possibility of interesting interactions due to the overlapping between doublet and quartet states.

A resemblance between spectra from the $a^4\Pi$ and $b^4\Sigma^-$ systems and the first bands of the O_2^+ molecule was noticed by Feast.[20] Later, attempts to formulate a Deslander table for

*Project supported by the Funds from Laser Sciences and Interactions Department, National Institute of Laser Enhanced Sciences (NILES), Cairo University, Giza, Egypt; the Fund from the Department of Physics, Faculty of Science for Girls, Imam Abdulrahman Ben Faisal University (x-Dammam University), the Fund from Dammam 31441, Saudi Arabia, and the Physics Department of King Fahd University of Petroleum and Minerals (KFUPM), Dhahran, Saudi Arabia.

†Corresponding author. E-mail: Ahmedasaad68@yahoo.com, Ahmedasaad@niles.edu.eg

© 2018 Chinese Physical Society and IOP Publishing Ltd

measuring transition was undertaken without being able to obtain a complete vibration analysis.[21,22]. Nonetheless at that time the assignment of Vichon *et al.*[23] was verified.

Möehlmann and Heer[24] reported that the experimental threshold energy for the observation of the $b^4\Sigma^-$–$a^4\Pi$ emission was 6.4 eV and they measured the lifetimes of the $b^4\Sigma^-$ ($\upsilon = 1,2$). A year Later Frueholz *et al.*[25] reported the quartet–doublet transitions $b^4\Sigma^-$–$X^2\Pi$ and $a^4\Pi$–$X^2\Pi$ by analyzing an electron-impact spectrum with accuracy up to 30 cm^{-1}. The electronic level of $a^4\Pi$ ($\upsilon = 0$) was found to be at 38250 cm^{-1} whereas the level $b^4\Sigma^-$ ($\upsilon = 0$) was assigned to be at 46120 cm^{-1}, above the $X^2\Pi$ ($\upsilon = 0$) level.

The formation of the $a^4\Pi$ and $b^4\Sigma^-$ states, as precursors to the population of the $B^2\Pi$ state, were investigated by Campbell and Mason.[26] This resulted in the reassignment of the vibration levels of the $b^4\Sigma^-$ state to give a dissociation energy of 275.6 ±1.6 K · J · Mol^{-1}. They reported that the highest observed level of the $b^4\Sigma^-$ is $\upsilon = 6$.

With the aim of locating the quartet states with respect to the doublet states, Miescher[27] studied the interactions between quartet and doublet states in the emission spectrum of NO molecule. Later, Huber and Vervloet[28] obtained the emission spectra of the $b^4\Sigma^-$–$a^4\Pi$ system of NO molecule by using a supersonic jet discharge. The spectrum covered the range from 750 nm to 2500 nm and a rotational analysis was performed. The relative positions of the quartet $b^4\Sigma^-$ and $a^4\Pi$ states were reevaluated to be $(a^4\Pi) = 38267.2 \pm 2$ cm$^-$ and $(b^4\Sigma^-) = 46171.8 \pm 2$ cm^{-1} relative to the $X^2\Pi$ ($\upsilon = 0$).

Bachir *et al.*[29] studied the intermolecular V–E transfer processes between molecules separated by a large distance and coupled by long range dipole–dipole interaction. They observed that these transfer processes induce the $b^4\Sigma^-$–$a^4\Pi$ electronic transition and reported the vibration lines $b^4\Sigma^-$ ($\upsilon = 0$–5)–$a^4\Pi$ ($\upsilon = 0$).

In the present work, we report on the fluorescence emission spectra of NO molecules excited using low power glow discharge under various experimental conditions such as gas pressures, buffer gases, NO concentrations, discharge voltage and time evolution of Ar/NO density ratio as well. This investigation will assist in understanding the interesting features of NO molecules such as collision processes, population dynamics and energy transfer within molecules. Furthermore, such an investigation can assist in developing new sensitive sensors that can monitor and track small quantities of NO diatomic molecule as a gas in air. To our knowledge, this is the first observation of a fluorescence emission spectrum of NO diatomic molecule excited by the low power glow discharge.

2. Experimental setup

Figure 1 shows the schematic diagram of the experimental setup of the CW gas discharge cavity tube with a length of 1 m and an 80% transmission output coupler for obtaining fluorescence emission spectrum of NO molecular gas via glow discharge.

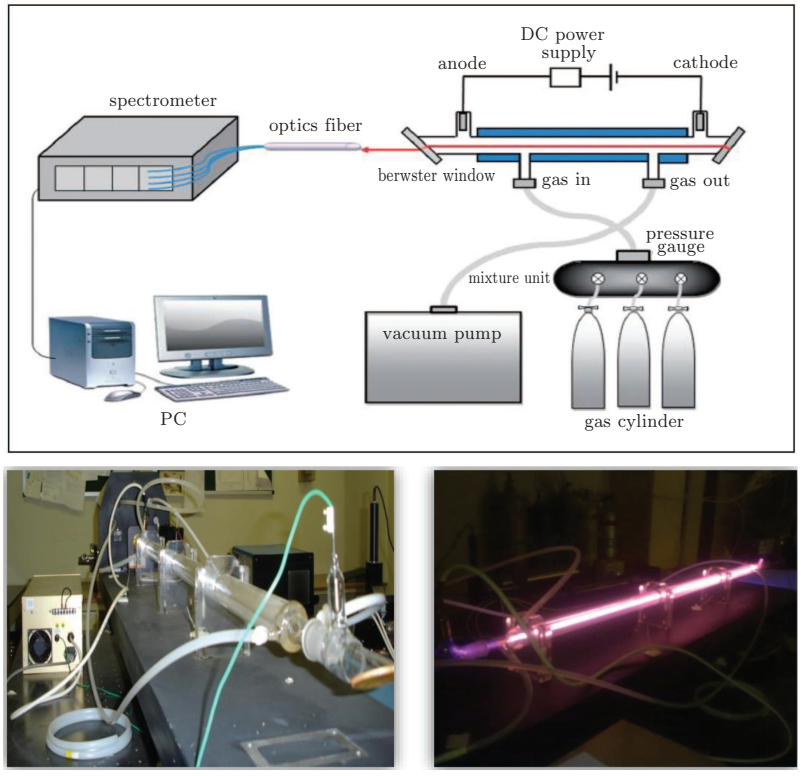


Fig. 1. (color online) Schematic diagram of experimental setup for obtaining emission spectrum of NO molecular gas (95% purity) at a pressure around 25 mbar via glow discharge voltage of 30 kV and current of 50 mA.

A special kind of glass cell, having four ports as shown in Fig. 2, was designed in our laboratory to create an electrical discharge for studying the fluorescence emission spectra of NO gas. The cell was initially evacuated using a rotary pump to prevent any contamination by atmospheric air. The cavity tube was then flushed with a purity of 95% NO diatomic gas at a specific pressure. It is worthy to mention that the optimum NO gas pressure conditions were accurately determined. The gas pressure around 25 mbar (1 bar = 10^5 Pa) was used. Both cathode and anode were made of steel and small pieces of tungsten wire of around 2-mm diameter, and they were screwed in the electrodes for connection with flowing tap water. The cathode cylinder and the anode pins were sealed inside the cavity tube and both were separated from each other by a distance of 120 mm. A water jacket with an outer diameter of 50 mm coaxially surrounded the central portion of the plasma tube with an internal diameter of 13 mm for the circulation of the chilled water for cooling the plasma tube. The tube was mounted on a wooden base with 200 mm in length, 120 mm in width, and 20 mm in height. The electric discharge tube included the gas flow at a low rate (1–20 litres per minute) In this work, A DC power supply of 30-kV discharge voltage and 50 mA was used to run the electrical discharge. Once the gas passed through the tube, the electrical discharge excited NO gas, resulting in the production of an emission spectrum.

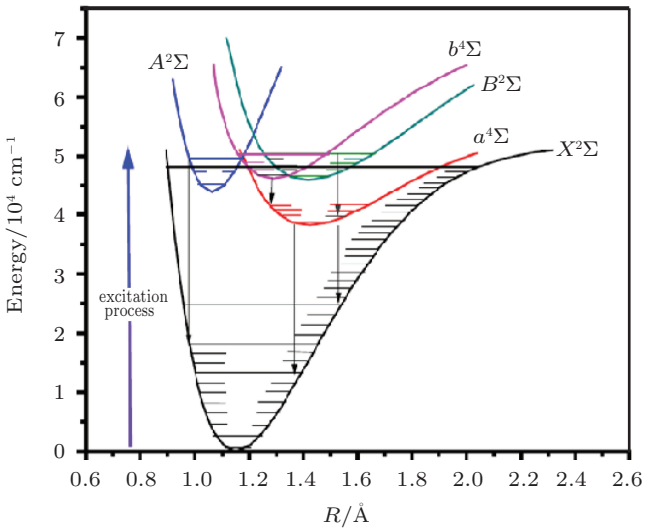


Fig. 2. (color online) Potential energy curves of the low lying quartet and doublet states of NO molecule vibrational states $A^2\Sigma$ ($\upsilon = 2$), $b^4\Sigma$ ($\upsilon = 3$), $B^2\Pi$ ($\upsilon = 4$), and $X^2\Pi$ ($\upsilon = 33$–32) all at a level of excitation energy.

The expected temperature inside the axial flow was 20 °C above the cooling water temperature. Whereas the cooling water temperature was fixed at 10 °C. The direct current (DC) power supply of 30 KV consisted of a 15-A Variac and a high voltage setup transformer. Longer bore led to the increase of the voltage for producing the discharge and the higher gas pressure needs more voltage for breakdown. Once the gas was passed, the current density per bore area could be recorded. The maximum current density was limited by the pump displacement

The fluorescence spectrum of the NO diatomic molecule was recorded using an Ocean Optics 2500+ spectrometer through a multimode UV graded fused silica (100-mm long) optical fiber with SMA connector. The data were transferred to an LIBS2500+ spectrometer (Ocean Optics) which contains seven spectrometer modules to provide high resolution (FWHM 0.1 nm) in the ultraviolet (UV) to near infrared (NIR) wavelength region. In this experiment, we used a gated CCD camera with 14336 pixels as a detector to record the emission spectrum over a broad band of spectra simultaneously with a high spectral resolution of 0.1 nm. The experimental setup for NO diatomic molecular spectrum is applicable for the investigation of more gas molecular spectra. It will be interesting process to extend such studies in our laboratory to a wide range of gases in the Periodic Table and discover some correlations with the molecular geometries of the objective gases.

3. Results and discussion

3.1. Line assignments and dissociation energy of NO

In this work, the fluorescence spectrum of NO diatomic molecule is observed in a wavelength range of 200 nm–1500 nm. In order to achieve correct assignment of the spectrum lines two steps are performed. The first step is to construct the potential energy curves of the doublet and quartet low energy states of NO molecule and the second step is to determine the allowed transitions and their assignments using a self- developed, special computer program (code)

The potential energy curves of the lower lying level of NO diatomic molecule are constructed using the Rydberg–Klein–Rees (RKR) method with the help of the Bound program of Foth *et al.*[30] Those states are $X^2\Pi$, $a^4\Pi$, $A^2\Sigma$, $B^2\Pi$, and $b^4\Sigma^-$. The essential spectroscopic constants required to construct the potential energy curves are cited from the literature[10,16–32] and are listed in Table 1.

By using the RKR method, the turning points of the vibration levels of the $X^2\Pi$, $a^4\Pi$, $A^2\Sigma$, $B^2\Pi$, and $b^4\Sigma^-$ states are listed in Tables 2–6, respectively. Figure 2 shows a schematic diagram of the potential energy curves of the lower lying doublet and quartet state of NO diatomic molecule The fluorescence experimental spectrum of NO obtained in the work is induced by the glow discharge system. Figure 2 shows that the vibration states $A^2\Sigma$ ($\upsilon = 2$), $b^4\Sigma^-$ ($\upsilon = 3$), $B^2\Pi$ ($\upsilon = 4$), and $X^2\Pi$ ($\upsilon = 33$–32) all lie in their corresponding level of the excitation energy. Therefore, these levels are populated by the glow discharge excitation energy, and emission lines originating from these levels of the ground state are observed.

Table 1. Spectroscopic constants (in unit cm^{-1}) for low lying doublet and quadric states of NO molecule.

		$b^4\Sigma$[28]	$B^4\Pi$[10]	$A^2\Sigma$[16]	$a^4\Pi$[28]	$X^2\Pi$[10]
Electronic term	T_e	48680	45942.6	43906.2	38440	0
Vibrational terms $\cong G_\upsilon$	Y_{10}	1262.354	1042.4	2374.37	1016.214	1904.13455
	Y_{20}	−14.797	−7.7726	−16.159	−10.313	−14.088358
	Y_{30}	0.0423	0.11596		−0.0259	0.0100467
	Y_{40}		-3.96×10^{-3}		-6.41×10^{-3}	-1.53×10^{-4}
	Y_{50}					-9.77×10^{-6}
	Y_{60}					-1.91×10^{-7}
	Y_{70}					-5.27×10^{-9}
Rotational terms $\cong B_\upsilon$	Y_{01}	1.3594	1.1244	1.9956	1.11677	1.70488847
	Y_{11}	−0.02002	−0.013433	−0.01871	−0.01485	−0.0175416
	Y_{21}	-1.91×10^{-4}	2.99×10^{-5}		-2.15×10^{-4}	0.00
	Y_{31}		-3.18×10^{-6}			0.00
	Y_{41}					-4.73×10^{-8}
	Y_{51}					1.01×10^{-9}
	Y_{61}					-6.06×10^{-11}

Table 2. Turning points of vibrational levels of $X^2\Pi$ state.

υ	$G(\upsilon)/cm^{-1}$	R_{min}/Å	R_{max}/Å
−0.50005	0	1.150783	1.150783
0.0	948.6466	1.104947	1.202649
1.0	2824.636	1.074751	1.245028
2.0	4672.534	1.055459	1.276675
3.0	6492.391	1.040623	1.304045
4.0	8284.249	1.028379	1.329007
5.0	10048.14	1.017878	1.352415
6.0	11784.1	1.00865	1.374748
7.0	13492.12	1.000401	1.396306
8.0	15172.21	0.992938	1.417293
9.0	16824.34	0.986119	1.437859
10.0	18448.46	0.979843	1.458116
11.0	20044.51	0.974032	1.478155
12.0	21612.39	0.968624	1.498051
13.0	23151.97	0.963571	1.517868
14.0	24663.08	0.958833	1.537664
15.0	26145.5	0.954379	1.557492
16.0	27598.98	0.95018	1.577402
17.0	29023.19	0.946214	1.597444
18.0	30417.77	0.942463	1.617669
19.0	31782.26	0.938909	1.63813
20.0	33116.14	0.935538	1.658881
21.0	34418.8	0.93234	1.679984
22.0	35689.54	0.929304	1.701506
23.0	36927.55	0.926422	1.723521
24.0	38131.9	0.923685	1.746116
25.0	39301.54	0.921088	1.769387
26.0	40435.28	0.918626	1.793448
27.0	41531.79	0.916293	1.818432
28.0	42589.55	0.914085	1.844496
29.0	43606.87	0.911998	1.871828
30.0	44581.88	0.910028	1.900656
31.0	45512.47	0.908168	1.931258
32.0	46396.32	0.90641	1.96398
33.0	47230.87	0.904743	1.999259

Strong spectral lines in the fluorescence spectrum are observed. Those lines are transited from the $A^2\Sigma$ ($\upsilon = 2$) vibration state to the ground $X^2\Pi$ ($\upsilon = 10$) state and from the $A^2\Sigma$ ($\upsilon = 0$) state to the $X^2\Pi$ ($\upsilon = 1$) state. The excitation of other doublet and quartet states observed by the spectral lines result from the transitions of the populated levels $b^4\Sigma^-$ ($\upsilon = 3$) and $B^2\Pi$ ($\upsilon = 4$) to the lower lying. Those transitions include the lines $b^4\Sigma^-$ ($\upsilon = 3$–0)–$a^4\Pi$ ($\upsilon = 0$), $b^4\Sigma^-$ ($\upsilon = 0$)–$a^4\Pi$ ($\upsilon = 1$), $B^2\Pi$ ($\upsilon = 4$–0)–$a^4\Pi$ ($\upsilon = 0$) and $B^2\Pi$ ($\upsilon = 0$)–$a^4\Pi$ ($\upsilon = 1$). The relaxing lines from the $a^4\Pi$ ($\upsilon = 0$) state to the ground state $X^2\Pi$ ($\upsilon = 7$, 15) are also identified.

Table 3. Turning points of vibrational levels of $a^4\Pi$ state.

υ	$G(\upsilon)/cm^{-1}$	R_{min}/Å	R_{max}/Å
−0.499963	0	1.42187	1.42187
0.0	505.4876	1.359681	1.493564
1.0	1500.959	1.319405	1.553328
2.0	2475.386	1.29408	1.598805
3.0	3428.305	1.274893	1.638841
4.0	4359.099	1.25929	1.676036
5.0	5266.997	1.246097	1.711612
6.0	6151.074	1.234653	1.746291
7.0	7010.253	1.224534	1.780568
8.0	7843.301	1.215442	1.814824
9.0	8648.831	1.207151	1.849386
10.0	9425.305	1.199478	1.884557
11.0	10171.03	1.192262	1.920645
12.0	10884.15	1.185355	1.957975
13.0	11562.68	1.17861	1.996918
14.0	12204.44	1.171873	2.03791
15.0	12807.15	1.164971	2.081484
16.0	13368.32	1.157698	2.128322
17.0	13885.36	1.149802	2.179322
18.0	14355.47	1.140949	2.235724
19.0	14775.75	1.130676	2.299316
20.0	15143.11	1.118304	2.372834

The glow discharge excites not only the doublet and quartet states, but also the higher vibrational levels of the ground state $X^2\Pi$ ($\upsilon = 33$, 32) of NO diatomic molecule. In this work, the transitions $X^2\Pi$ ($\upsilon = 33$)–$X^2\Pi$ ($\upsilon = 15$, 17, 20) and $X^2\Pi$ ($\upsilon = 32$)–$X^2\Pi$ ($\upsilon = 18$) are well identified. Those transi-

tions have high intensity in the 400 nm–800 nm region. To our knowledge, none of those new lines obtained experimentally has been reported in the literature.

Table 4. Turning points of vibrational levels of $A^2\Sigma$ state.

υ	$G(\upsilon)/\text{cm}^{-1}$	$R_{\min}$/Å	$R_{\max}$/Å
−0.50002	0	1.063665	1.063665
0.0	1183.184	1.022494	1.109963
1.0	3525.236	0.995217	1.147588
2.0	5834.97	0.977711	1.175567
3.0	8112.386	0.964196	1.199684
4.0	10357.48	0.953001	1.221613
5.0	12570.26	0.943364	1.242122
6.0	14750.73	0.934861	1.261635
7.0	16898.87	0.92723	1.280421

Table 5. Turning points of vibrational levels of $B^4\Pi$ states.

υ	$G(\upsilon)/\text{cm}^{-1}$	$R_{\min}$/Å	$R_{\max}$/Å
−0.499965	0	1.417035	1.4170345
0.0	519.6047	1.355358	1.4874414
1.0	1546.817	1.315141	1.5452583
2.0	2559.412	1.289685	1.5885212
3.0	3557.897	1.270291	1.6259401
4.0	4542.682	1.254446	1.6600389
5.0	5514.084	1.241009	1.6919739
6.0	6472.322	1.229346	1.7223946
7.0	7417.523	1.219063	1.7517147

Table 6. Turning points of vibrational levels of $b^4\Sigma$ state.

υ	$G(\upsilon)/\text{cm}^{-1}$	$R_{\min}$/Å	$R_{\max}$/Å
−0.49997	0	1.288748	1.288748
0.0	627.4384	1.233233	1.353434
1.0	1860.336	1.197581	1.407851
2.0	3064.02	1.175292	1.449487
3.0	4238.745	1.158491	1.486238
4.0	5384.764	1.144914	1.520394
5.0	6502.331	1.133534	1.553006
6.0	7591.7	1.123789	1.584663
7.0	8653.125	1.115331	1.615744

In addition, few strong sharp lines of NO diatomic molecule are observed in the 600 nm–700 nm spectral region. Those lines prove that the presence of atomic lines of oxygen (630 nm) line and nitrogen atoms. Some weak lines are observed at 709 nm and 619 nm of O and N atoms, respectively.

Table 7 lists the fluorescence emission molecular lines produced by the excitation glow discharge in this work. Figure 3 shows the assignments of these lines in the spectral region at fixed 30-kV glow discharge voltage, 25-mbar NO gas pressure, and 50-mA discharge current. In Fig. 3, it can be noticed that the (3–0) transition of $b^4\Sigma^-$–$a^4\Pi$ system and the (4–0) transition of $B^2\Pi$–$a^4\Pi$ system have high intensity due to the overlapping of emission lines in that region as a result of the levels $b^4\Sigma^-$ ($\upsilon = 3$) and $B^2\Pi$ ($\upsilon = 4$) being in the same proximity of energy as can be seen from the RKR curves in Fig. 2.

Table 7. Observed lines and assignment of the fluorescence spectrum of NO in region of 200 nm–1500 nm.

System	(υ', υ)	λ/nm	System	(υ', υ)	λ/nm
$A^2\Sigma$–$X^2\Pi$	(0,1)	237.02	$X^2\Pi$–$X^2\Pi$	(33,15)	474.26
	(2,0)	320.11		(33,17)	549.22
$a^4\Pi$–$X^2\Pi$	(0,7)	395.56		(32,18)	625.84
	(0,15)	791.94		(33,20)	708.48
$B^2\Pi$–$a^4\Pi$	(4,0)	867.56	$b^4\Sigma^-$–$a^4\Pi$	(3,0)	868.52
	(3,0)	948.34		(2,0)	954.18
	(2,0)	1047.14		(1,0)	1109.99
	(1,0)	1184.9		(0,0)	1269.62
	(0,0)	1343.43		(0,1)	1424.39

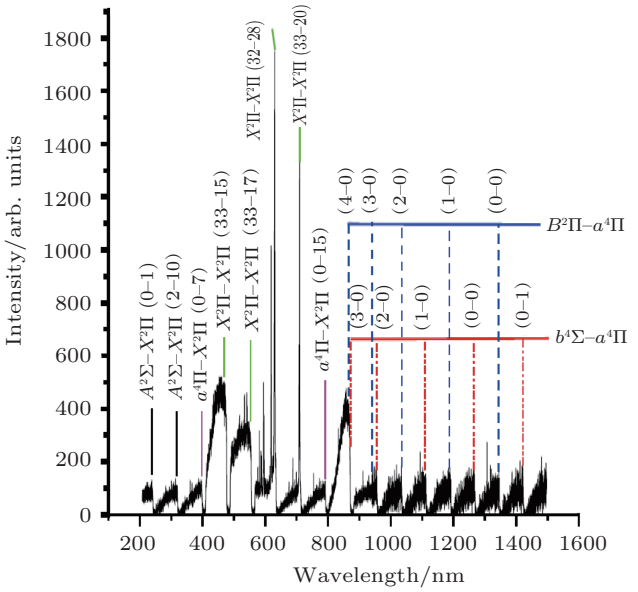


Fig. 3. (color online) Fluorescence spectra of NO diatomic molecules in the UV to NIR spectral region. The line assignments made for transitions $X^2\Pi$–$X^2\Pi$ (33–15), $X^2\Pi$–$X^2\Pi$ (33–17), $X^2\Pi$–$X^2\Pi$ (33–20), and $X^2\Pi$–$X^2\Pi$ (33–18) respectively at fixed 30-kV glow discharge voltage, 25-mbar NO gas pressure, and 50-mA discharge current.

In order to determine the dissociation energy of the NO diatomic molecule, the top of vibration levels in the ground $X^2\Pi$ state have been investigated using our experimental spectrum in this work The line assignments made for the transitions $X^2\Pi$–$X^2\Pi$ (33–15), $X^2\Pi$–$X^2\Pi$ (33–17), $X^2\Pi$–$X^2\Pi$ (33–20), and $X^2\Pi$–$X^2\Pi$ (33–18) respectively have been analyzed. The energy values for the vibration levels $\upsilon = 32$ and 33 for the ground $X^2\Pi$ state are determined to be 46294.96 cm^{-1} and 47203.02 cm^{-1}, respectively. Therefore, it can be able to calculate the dissociation energy of the ground state of NO diatomic molecule by using the Birge–Sponer method. Whereas, the difference in energy between vibration energy levels on the vertical axis and the vibration quantum number on the horizontal axis is exactly plotted. The intersection of the extrapolated curve with the horizontal axis gives the highest vibration quantum number and the dissociation level.

The highest vibration level of the ground $X^2\Pi$ state is reported at $\upsilon' = 22$. We use the experimental values for levels $\upsilon' = 0$–22 and the calculated values for the higher vibration levels $\upsilon' = 32$–33 (see below) to perform the Birge–Sponer extrapolation method The dissociation energy of the NO molecule is found to be 51336 cm^{-1} at level $\upsilon'_{\max} = 44$ with D_0. This is in agreement with the value reported in Ref. [14].

3.2. Temporal development of NO molecular density

The time evolution of the fluorescence intensity of NO molecular density in the post-discharge region of NO/O_2/Ar mixture at various argon gas concentrations, Ar (1%)/NO, Ar (5%)/NO, Ar (10%)/NO, and Ar (20%)/NO at fixed 30-kV glow discharge voltage and 50-mA discharge electric current are depicted in Fig. 4. The NO concentration is adjusted by the mixing ratio of NO/O_2/Ar gas, measured with an NO_x analyzer. It is observed that the fluorescence intensity of the initial NO density decreases with increasing argon concentration at a fixed time of 60 μs. The reduction in density can be attributed to the variation of the discharge power. The negative gas like oxygen (O_2) may diminish the electron mean energy which leads to less NO yield. The NO molecules decays monotonically after discharge pulse at a constant time ($t = 65$ μs) which may be due to the diffusion from the observation volume and/or recombination between plasma species.

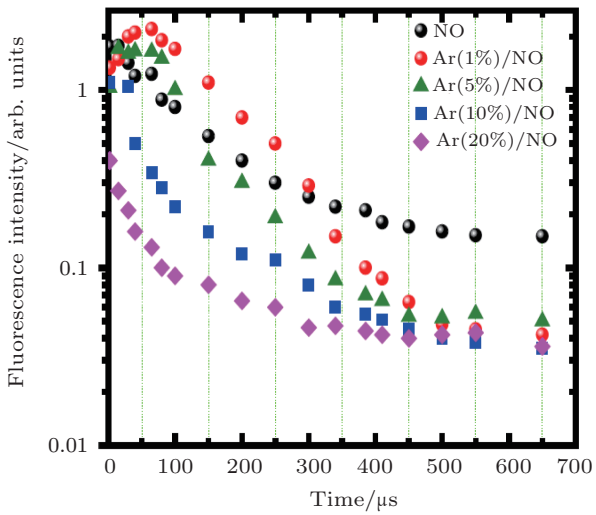


Fig. 4. (color online) Time evolution of fluorescence intensity of NO molecular density in the post-discharge region of NO molecular gas relative to argon gas mixture in the probed state after glow discharge at various argon ambient gas concentrations Ar (1%)/NO, Ar (5%)/NO, Ar (10%)/NO, and Ar (20%)/NO at fixed 30-kV glow discharge voltage, 25 mbar, and 50 mA.

The decay saturation of NO diatomic molecule may be due to "ozone interference".[33] The glow discharge dissociates ozone into O (^{1}D) radical and O_2, which react with NO to form NO_2. Therefore, the photo-dissociation of ozone tends to raise the NO-fluorescence intensity. In addition, the decay saturation behavior in Fig. 4 might be caused by photo-dissociation of long-lived molecules such as HNO_x like ozone interference. The lower limit of NO density can be determined by fluorescence process if the ozone interference is present.

3.3. Dependence of fluorescence signal intensity on NO molecular gas concentration

The fluorescence signal intensity depends on the number of the particles "N" of NO molecules excited to the higher state "j" which is de-excited to lower state "i" to emit the radiation spectrum. Figure 5 shows the variations of the fluorescence intensity of the emission lines of NO diatomic molecules with the percentage of NO molecular gas concentration, respectively, at different discharge electric current values of 10, 30, 50, 80, and 100 mA with glow discharge voltage fixed at 30 kV in the glow discharge. The temperature in the cavity tube is kept at 40 °C. The fluorescence intensity varies from 40 to 130 arbitrary units (a.u.) for 10 mA, from 150 a.u. to 425 a.u. for 30 mA, from 235 a.u. to 670 a.u. for 50 mA, from 330 a.u. to 950 a.u. for 80 mA, and from 300 a.u. to 1290 a.u. for 100 mA. For each NO molecular gas concentration, the average spectrum is recorded.

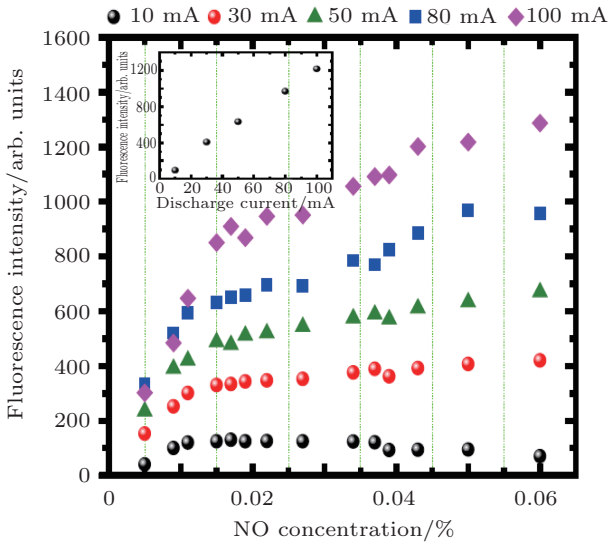


Fig. 5. (color online) Variation of the fluorescence intensity from the emission lines of NO molecule with percentage of NO molecular gas concentration at different discharge electric current values of 10, 30, 50, 80, and 100 mA, a fixed glow discharge voltage at 30 kV in the glow discharge and 25-mbar NO gas pressure. The temperature in cavity tube is kept at 40 °C.

It is observed that at lower NO molecular gas concentration, the fluorescence intensity increases slowly and then follows on a faster scale toward the saturation. The variation in the fluorescence intensity is affected by increasing the NO molecular gas concentration. This means that more exciting molecular species are produced, hence the fluorescence intensity increases. At higher NO molecular gas concentration the

dense plasma is produced and the fluorescence intensity is saturated which may be due to plasma shielding. Whereas the free electrons in the plasma could not absorb more energy coming from the glow discharge emitted light and the saturation of the fluorescence intensity will occur. The relationship between excitation power in fluorescence measurements and fluorescence intensity can be complicated. It is worthy to mention that at high excitation power, the saturation effects can occur where the excited states of fluorescent molecules are depopulated during stimulated emission[34] or those molecules are photobleached.[35] If dense plasma is formed, this means that the higher electron density is produced and high energy is transferred to the background gas (NO) to produce a larger number of excited NO molecules, and then higher emission spectra are emitted. While at low excitation energy, fluorophores may not exhibit fluorescence at all.[36] Hence, the excitation radiation power can possibly have a large influence on the intensity of fluorescence light measured.

3.4. Dependence of fluorescence intensity on applied discharge voltage

The influence of applied discharge voltage on fluorescence intensity of NO molecules is studied. Figure 6 shows the dependence of NO molecular gas on applied discharge voltage (13 kV–37 kV) in the glow discharge with the electric current fixed at 50 mA. It can be seen that the fluorescence intensity of NO molecule increases linearly with applied discharge voltage increasing. It is worth mentioning that a high- discharge voltage efficiently produces high emissions. The current passing through the electric discharge is measured to estimate the discharge power precisely. A lot of efforts are still made to determine the discharge power in future work. This study could be useful for better understanding the chemical and physical process occurring in the glow discharge plasma.

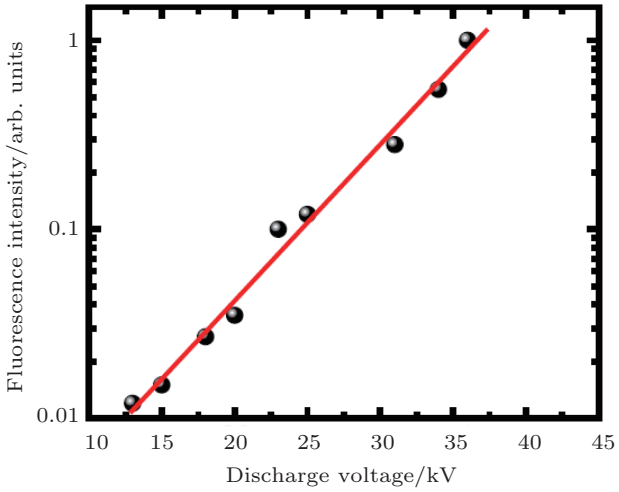


Fig. 6. (color online) Dependence of fluorescence intensity on applied discharge voltage (in a range of 13 kV–37 kV) in the glow discharge, with pressure fixed at 25 mbar and electric current at 50 mA.

4. Conclusions

In this work, the NO diatomic molecular spectrum is investigated by using a glow discharge as an excitation source. The NO fluorescence intensity is studied in a glow discharge plasma. The fluorescence spectrum is recorded in the ultraviolet, UV — near infrared, NIR region. Using the potential energy curves for the different electronic states of NO diatomic molecule in the proximity of the glow discharge energy, an explanation of the most probable transitions is suggested. For the recorded spectra of NO diatomic molecule, the line assignments are performed, which includes the transitions from higher doublet and quartet states to the ground state. Moreover, strong lines are observed in a region of 500 nm–800 nm which is assigned to vibration transition from the $\upsilon = 32$–33 levels to lower level in the $X^2\Pi$ state. These vibration levels are near to the dissociation energy of NO ground state; hence a more accurate evaluation of the dissociation energy of the ground state is performed. To the best of our knowledge, some of the transitions reported in this work have not been reported previously in the literature. Moreover, the value calculated from the dissociation energy of the ground state of NO diatomic molecule is more accurate as it includes the information about the highest vibration energy levels of this state. The influence of Ar and NO molecular gas concentration, and applied discharge voltage on the fluorescence intensity are also studied by using the fluorescence of the glow discharge. It is depicted that the fluorescence process is a promising diagnostic technique for recording the NO molecular spectrum in glow discharge.

References

[1] Cohen M F, Mazzola M and Yamasaki H 2006 "Nitric Oxide Research in Agriculture", in *Bridging the Plant and Bacterial Realms*, eds. Ashwani K Rai and Teruhiro Takabe (The Netherlands: Springer Press) p. 71
[2] Corker H and Poole R K 2003 *J. Biol. Chem.* **278** 31584
[3] D Serca, R Delmas, Le Roux X, Parsons D A B, Scholes M C, Abbadie L, Lensi R, Ronce O and Labroue L 1998 *Global Biogeochemical Cycles* **12** 637
[4] McClenny W A, Williams E J, Cohen R C and Stutz J 2002 *J. Air and Waste Manage. Assoc.* **52** 542
[5] Knowles G and Moncada S 1994 *Biochem. J.* **298** 249
[6] Moncada S, Palmer R M J and Higgs E A 1991 *Pharmacol Rev.* **43** 109
[7] Dingle T W, Freedman P A, Gelernt B, Jones W J and Smith I W M 1975 *Chem. Phys.* **8** 171
[8] Dünnwald H, Siegel E and Urban W 1985 *Chem. Phys.* **94** 195
[9] Rottke H and Zacharias H 1985 *J. Chem. Phys.* **83** 4831
[10] Luque J and Crosley D R 1995 *J. Quantum Spectrosc. Radiat. Transfer* **53** 89
[11] Brunger M J, Campbell L, Cartwright D C, Middleton A G, Mojarrabi B and Teubner P J O 2000 *J. Phys. B: At. Mol. Opt. Phys.* **33** 809
[12] Zhang G, Jin W and Zhang H 2013 *J. Quantum Spectrosc. Rad. Transfer* **127** 90
[13] Takazawa K 2004 *J. Mol. Spectrosc.* **223** 120
[14] Reddy R R, Ahammed Y N, Basha D B, Narasimhulu K, Reddy L S S and Gopal K R 2006 *J. Quantum Spectrosc. Rad. Transfer* **97** 344

[15] Poland H M and Broida H P 1971 *J. Quantum Spectrosc. Rad. Transfer* **11** 1863
[16] Danielak J, Domin U, Kepa R and Zachwieja M R 1997 *J. Mol. Spectrosc.* **181** 394
[17] Simeonsson J B, Elwood S A, Niebes M, Carter R and Peck A 1999 *Analy. Chim. Acta* **397** 33
[18] Mitscherling C, Maul C, Veselov A A and Gericke K H 2009 *Isotopes in Environmental and Health Studies* **45** 59
[19] Diez-Y-Riega H and Eilers H 2012 *Appl. Phys. B* **108** 189
[20] Khalil A A I, Morsy M A and El-Deen H Z 2017 *Opt. Laser Technol.* **96** 227
[21] Khalil A A I, Hafez A I, Elgohary M E and M A Morsy 2017 *Chin. Phys. B* **26** 095201
[22] Brook M and Kaplan J 1954 *Phys. Rev.* **96** 1540
[23] Vichon D, Hall R I, Gresteau F and Mazeau J 1978 *J. Mol. Spectrosc.* **69** 341
[24] Möhlmann G R and DeHeer F J 1977 *Chem. Phys. Lett.* **49** 588
[25] Frueholz R P, Rianda R and Kuppermann A 1978 *J. Chem. Phys.* **68** 775
[26] Campbell I M and Mason R S 1979 *J. Photochem.* **11** 53
[27] Miescher E 1980 *J. Chem. Phys.* **73** 3088
[28] Huber K P and Vervloet M 1988 *J. Mol. Spectrosc.* **29** 1
[29] Bachir H, Charneau R and Dubost H 1993 *Chem. Phys.* **177** 675
[30] Foth H J, Polanyi J C and Telle H H 1982 *J. Phys. Chem.* **86** 5027
[31] Khalil A A I, Younis W O and Gandol M A 2017 *Indian J. Phys.* **91** 327
[32] Al-Tuwirqi R, Al-Suliman N, Khalil A A I and Gandol M 2012 *Mol. Phys.* **110** 2951
[33] Wang C C, Davis L I Jr, Wu C H and Japar S 1976 *Appl. Phys. Lett.* **28** 14
[34] Georges J, Arnaud N and Parise L 1996 *Appl. Spectrosc.* **50** 1505
[35] Faris G W, Copeland R A, Mortelmans K and Bronk B V 1997 *Appl. Opt.* **36** 958
[36] Kaye P, Stanley W R, Hirst E, Foot E V, Baxter K L and Barrington S J 2005 *Opt. Express* **13** 3583